

UMONS

Université de Montpellier

materials

UMONS RESEARCH INSTITUTE
FOR MATERIALS SCIENCE
AND ENGINEERING

CIRMAP

UMONS Research Institute
for Materials Science
and Engineering

CMN

UMONS Research Institute
for Materials Science
and Engineering

Mesures quantitatives des
propriétés mécaniques de
matériaux mous

Philippe LECLERE

GT Nanomécanique
October 16, 2018
Montpellier (France)

REMISOL

UMONS

Université de Montpellier

Outline

Introduction – Scanning Probe Microscopy

Beyond imaging the morphology ...

... Mechanical Properties

Sub Resonance Tapping

Intermodulation AFM

Back to Contact Resonance

Conclusions

REMISOL

UMONS

Université de Montpellier

Imaging Modes

Contact mode

Non-contact mode

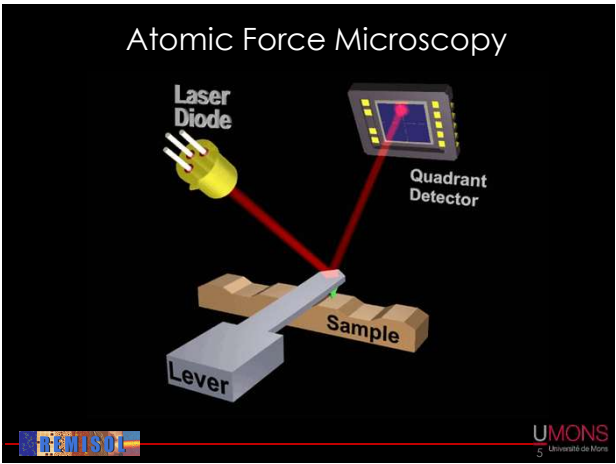
Intermittent contact

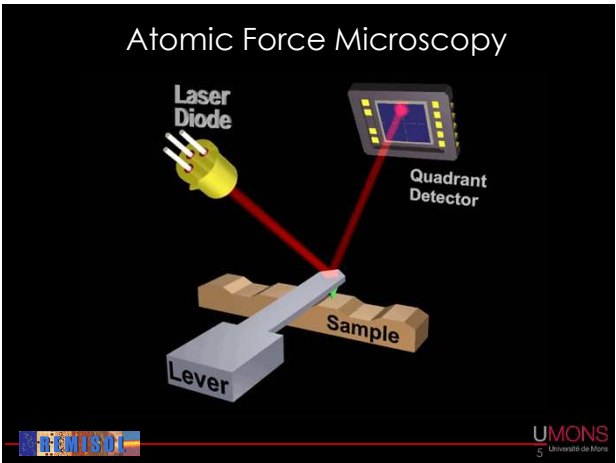
Force modulation mode

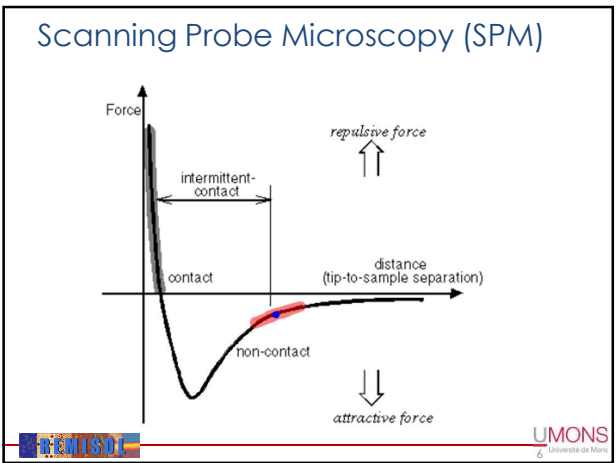
REMISOL

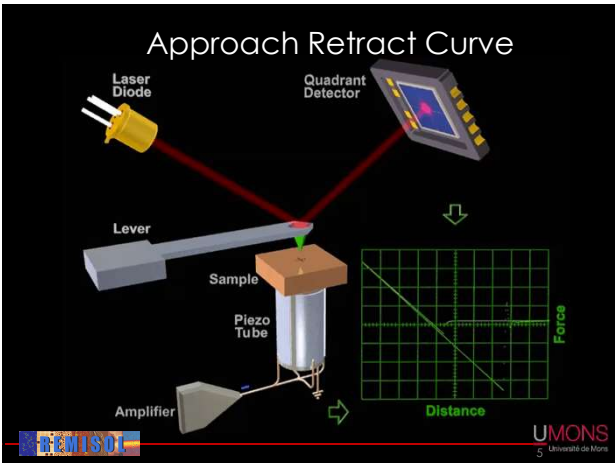
UMONS

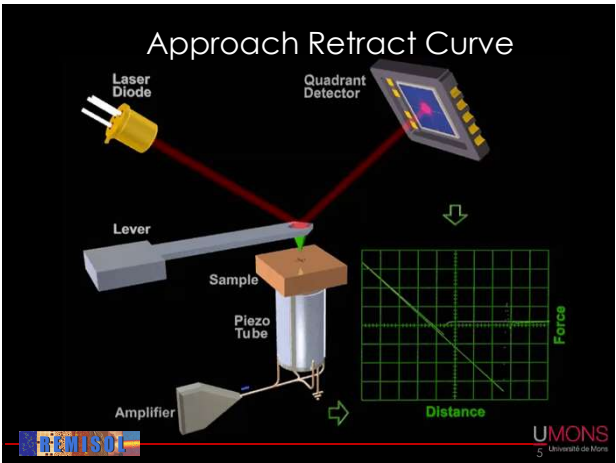
Université de Montpellier

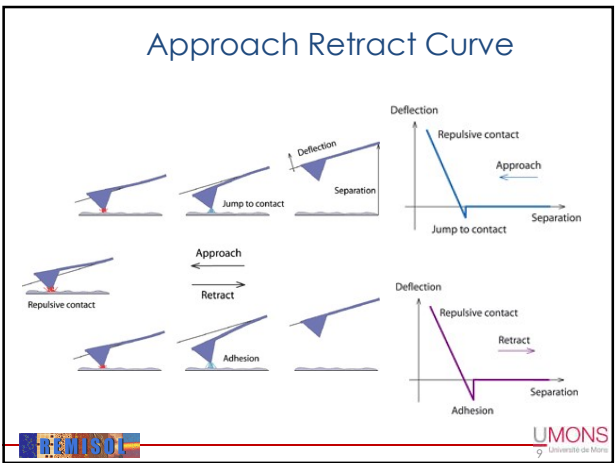




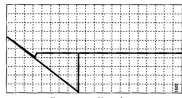




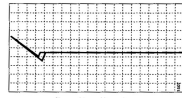




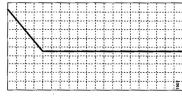
Approach Retract Curve



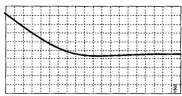
Large adhesion



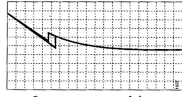
Small adhesion



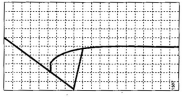
Hard sample



Soft sample



Long-range repulsion

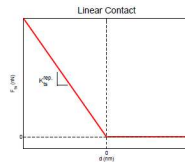


Long-range attraction



UMONS
Université de Mons

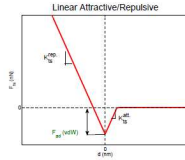
Models for tip-sample interactions



$$F_{LC}(d) = \begin{cases} 0, & d > 0 \\ -k_0^L d, & d \leq 0 \end{cases}$$

VEDA: A web-based virtual environment for dynamic atomic force microscopy

Tip-sample force versus gap for the piecewise linear contact model.



$$F_{LAR}(d) = \begin{cases} 0, & d < L_0 \\ k_0^L(d - L_0), & L_0 < d < 0 \\ -k_0^L d, & d \geq 0 \end{cases}$$

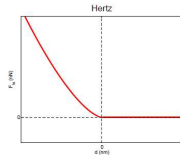
Tip-sample force versus gap for the piecewise linear attractive/repulsive contact model.



Review of Scientific Instruments 79, 061301 (2008)

UMONS
Université de Mons

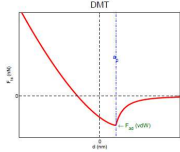
Models for tip-sample interactions



$$F_H(d) = \begin{cases} 0, & d > 0 \\ \frac{4}{3} E^* \sqrt{R} (-d)^{3/2}, & d \leq 0 \end{cases}$$

$$E^* = \left[\frac{1 - \nu_{tip}^2}{E_{tip}} + \frac{1 - \nu_{sample}^2}{E_{sample}} \right]^{-1}$$

Tip-sample force versus gap for the Hertz contact model.



$$F_{DMT}(d) = \begin{cases} -\frac{H}{d}, & d > a_0 \\ -\frac{H}{d} + \frac{4}{3} E^* \sqrt{R} (a_0 - d)^{3/2}, & d \leq a_0 \end{cases}$$

$$E^* = \left[\frac{1 - \nu_{tip}^2}{E_{tip}} + \frac{1 - \nu_{sample}^2}{E_{sample}} \right]^{-1}$$

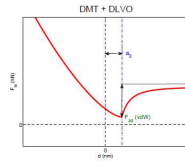
H = Hamaker constante



Review of Scientific Instruments 79, 061301 (2008)

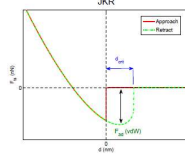
UMONS
Université de Mons

Models for tip-sample interactions



$$F_{\text{DLVO+DMT}}(d) = \begin{cases} \frac{d^2 B}{\cos K C} \gamma \gamma_{\text{spec}} K d - \frac{d^2 B}{\cos K C} & d > d_0 \\ \frac{d^2 B}{\cos K C} \gamma \gamma_{\text{spec}} K d - \frac{d^2 B}{\cos K C} + \frac{1}{2} E^* \sqrt{R} (d_0 - d)^{3/2}, & d \leq d_0 \end{cases}$$

$$E^* = \left[\frac{1 - \nu_{\text{tip}}^2}{E_{\text{tip}}} + \frac{1 - \nu_{\text{sample}}^2}{E_{\text{sample}}} \right]^{-1}$$

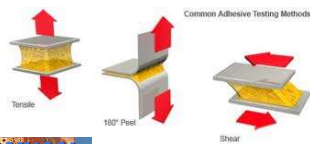


JKR is nonconservative and includes a dependency to the history of the tip-sample contact



UMONS
13 Université de Mons

Mechanical Properties



UMONS
14 Université de Mons

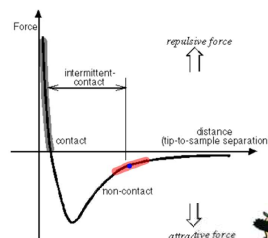
Scanning Probe Microscopy (SPM)

Morphology

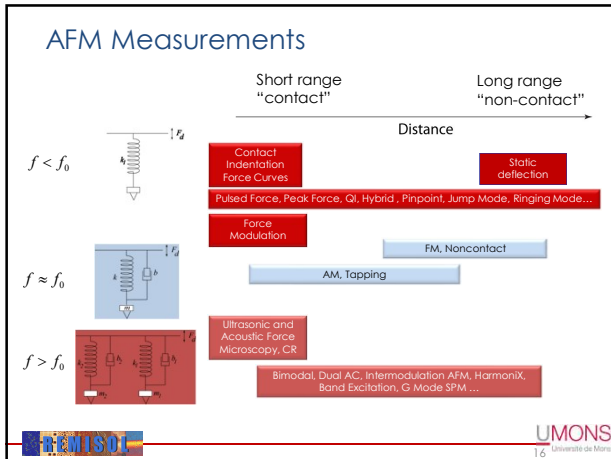
- Contact AFM
- AM-AFM (Tapping Mode)
- FM-AFM (nc-AFM)

Mechanical Properties

- Friction Force Microscopy
- Force Modulation
- Contact Resonance
- HarmoniX
- Bimodal Dual AC
- Peak Force Tapping
- Intermodulation AFM
- Band Excitation
- ...



UMONS
15 Université de Mons



What do we need ?

- A proper calibration of the AFM and the probe**
 - scanner, photodetector sensitivities** : approach-retract curve on stiff sample (silicon, sapphire, ...)
 - probe**: spring constant, resonance frequency, quality factor, tip geometry and dimension (electron microscopy or tip shape reconstruction).
- A suitable contact mechanics model**
 - DMT model, JKR model, Sneddon model, ...
- A signal giving access to the tip-surface contact stiffness**
 - "slope" of force-curve in the contact region,
 - modulated cantilever vibration,
 - phase-shift in AM-AFM,
 - contact resonance frequency,
 - higher harmonics vibration amplitude,
 - In phase and quadrature signals, ...



UMONS 17 Université de Mons

Contact Mechanics Forces

Basic Hertz's elastic solution (1881)

The figure shows the Hertzian contact stress distribution, which is a semi-elliptical shape with a maximum stress at the center of the contact area. It also includes a small diagram of a sphere in contact with a flat surface and a portrait of Heinrich Hertz.

UMONS 18 Université de Mons

Solid-state deformations

Several classes of deformations in elastic materials are the following:

Elastic: The material recovers its initial shape after deformation.

Anelastic: if the material is close to elastic, but the applied force induces additional time-dependent resistive forces (i.e. depend on rate of change of extension/compression, in addition to the extension/compression).

Viscoelastic: If the time-dependent resistive contributions are large, and cannot be neglected. Rubbers and plastics have this property, and certainly do not satisfy Hooke's law. In fact, elastic hysteresis occurs.

Plastic: The applied force induces non-recoverable deformations in the material when the stress (or elastic strain) reaches a critical magnitude, called the yield point.

Hyperelastic: The applied force induces displacements in the material following a strain energy density function.



Contact Mechanics Forces

To determine the deformation of two elastic objects in contact, we have to establish and resolve the relationship between the stress and strain tensors. This functional relationship is called the **constitutive equation**.

$$\Gamma_{ij} = \lambda \epsilon_{ij} \delta_{ij} + G \epsilon_{ij}$$
 λ is the Lamé coefficient

The **shear modulus** G is given by :

$$G = \frac{E}{2(1+\nu)}$$

At equilibrium, the **elasticity parameter**

$$\lambda_e = \Gamma_0 \left(\frac{9R}{2\pi W_{ad} E_{eff}} \right)^{1/3}$$

W_{ad} is the work per unit of area required to fully separate the surfaces

$$\frac{1}{E_{eff}} = \left(\frac{1-\nu_t^2}{E_t} + \frac{1-\nu_s^2}{E_s} \right)$$

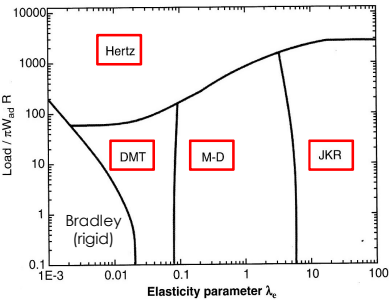
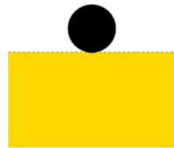


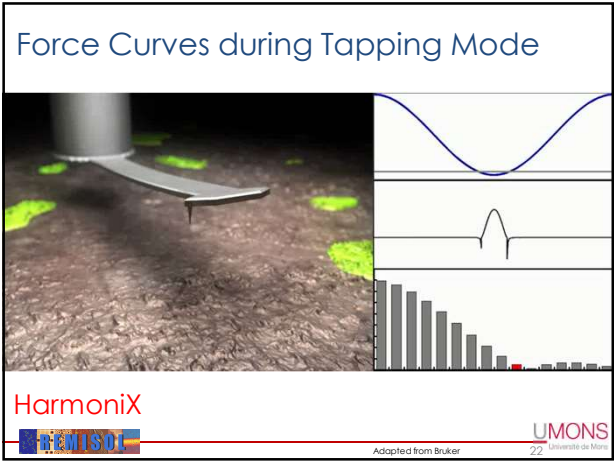
Contact Mechanics Forces

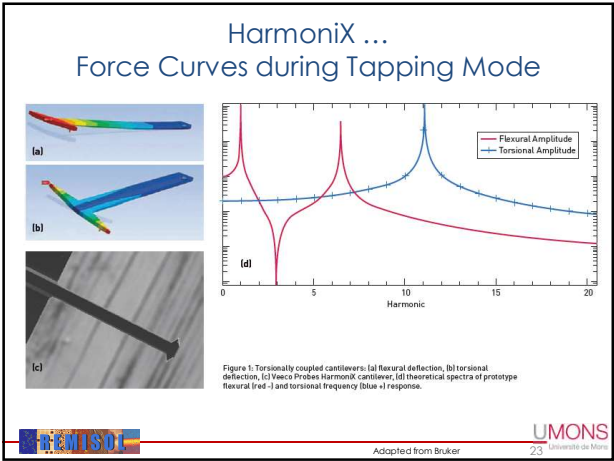
DMT = Dejarguin – Muller – Toporov (stiff contacts, low adhesion)

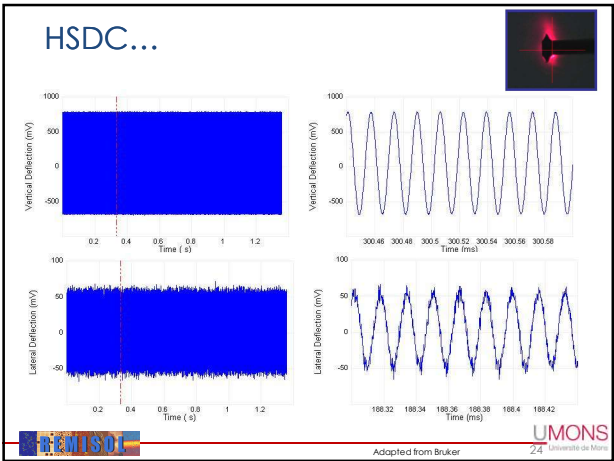
M-D = Maugis - Dugdale

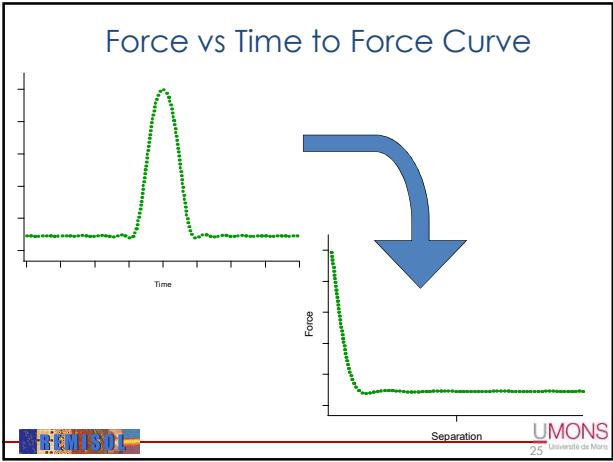
JKR
Johnson – Kendall – Roberts
(low stiffness, high adhesion,
large tip)

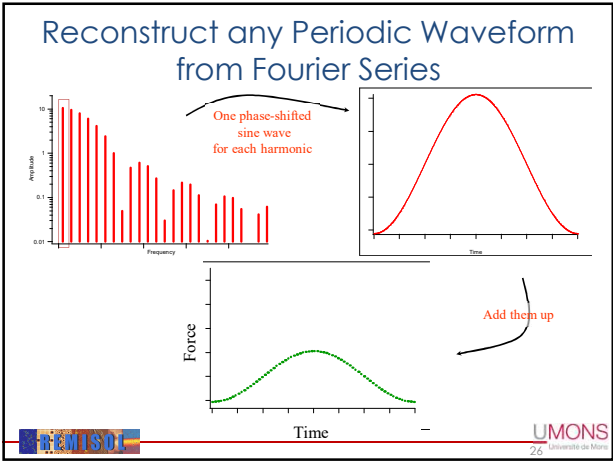


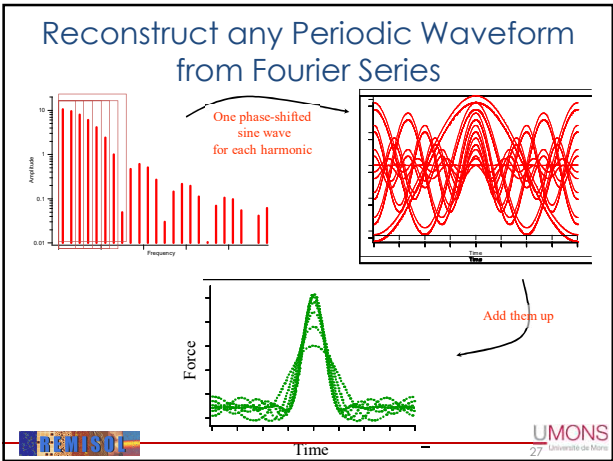


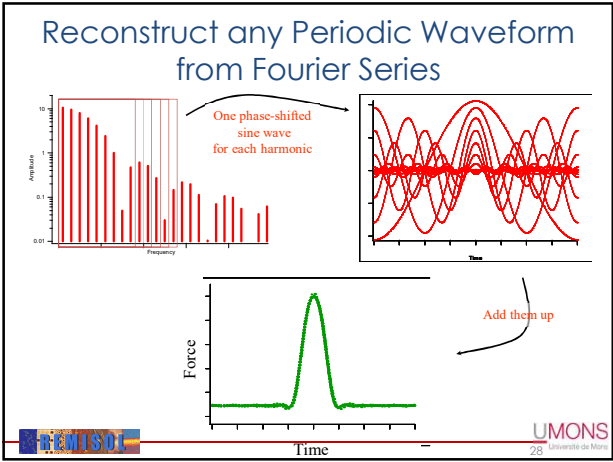


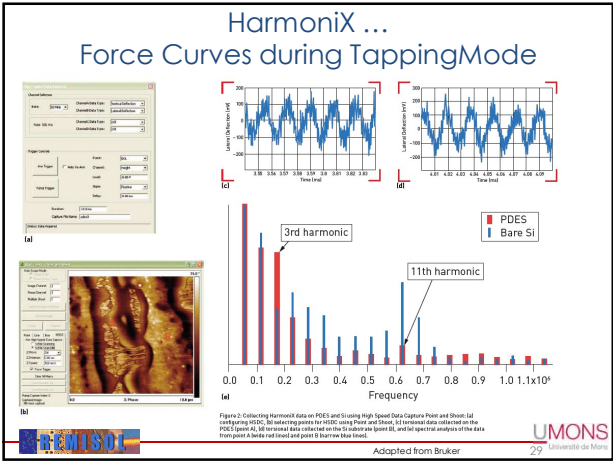


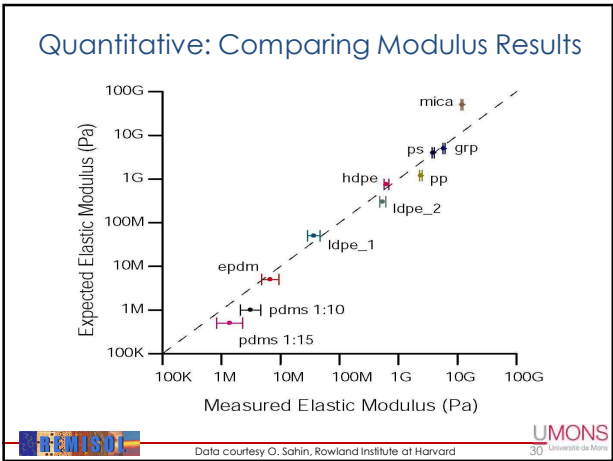


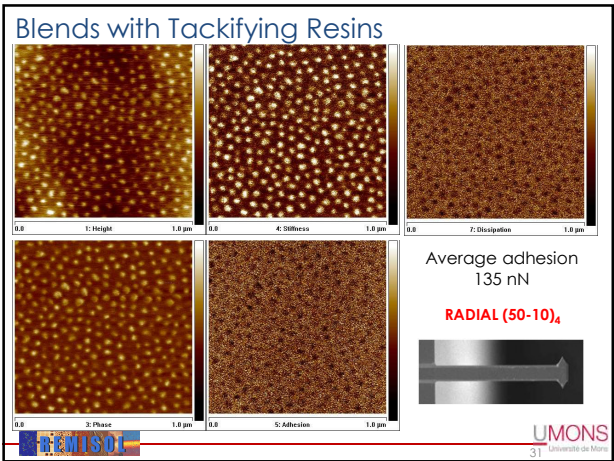






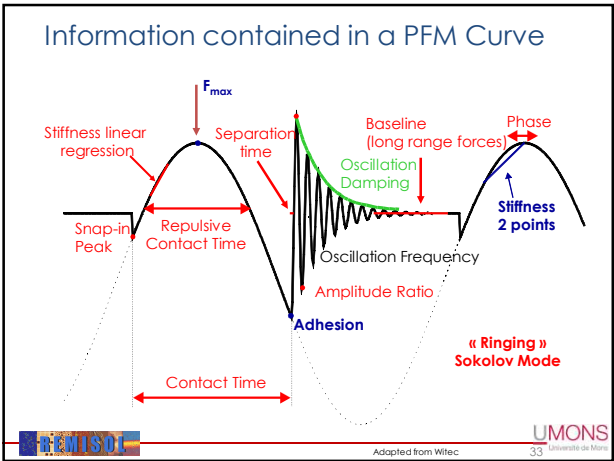






Sub Resonance Tapping

aka PeakForce Tapping, Jump Mode, Hybrid™, Pinpoint™, QI™, « Ringing » Mode AFM, ...



Comparing various modes when imaging of soft materials with AFM

	Contact	Tapping	Sub-resonance
Contact area	Unstable contact	Small but hard to control	Small
Lateral Resolution	Low	Good*	Good*
Friction artifacts	Stick-slip	Minimum to none	Minimum to none
Sample safe	Potentially destructive	Non-destructive	Non-destructive
Force control	Excellent	Hard to control	Good
Quantitative physical info	Yes (force-volume mode)	No	Yes**

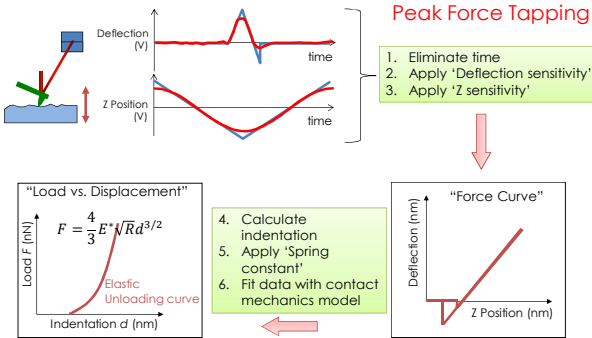
* Depends on material
** Accuracy is yet to be verified



UMONS
Université de Mons

Analyzing Force Curves

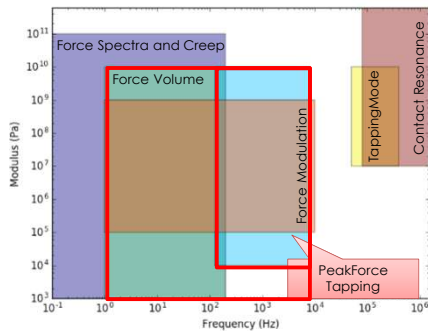
From Deflection and Z to modulus



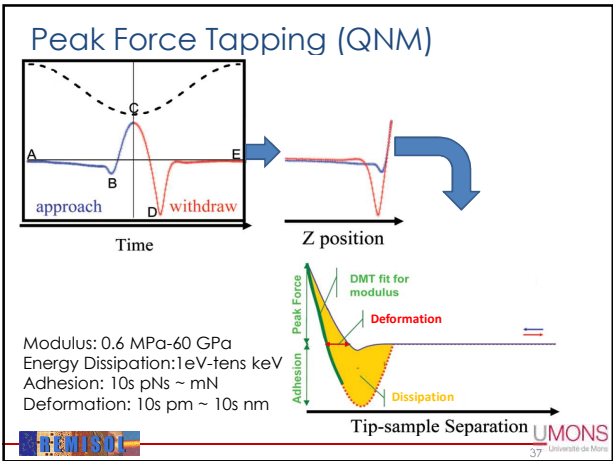
Adapted from Bruker

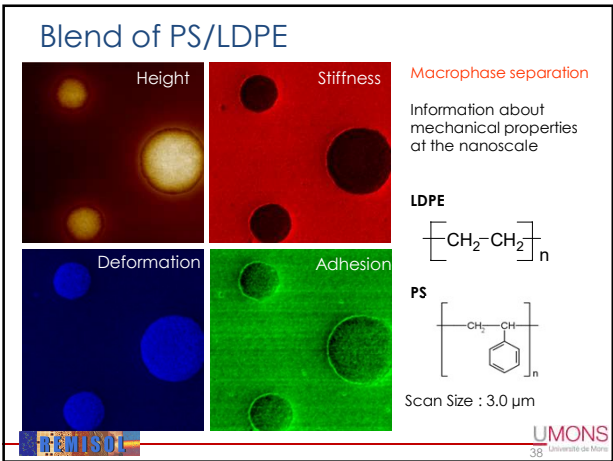
UMONS
Université de Mons

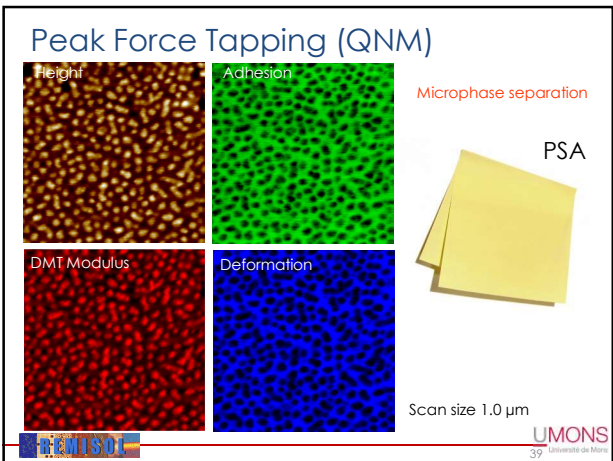
AFM frequency and modulus ranges
Force Volume and PeakForce Tapping



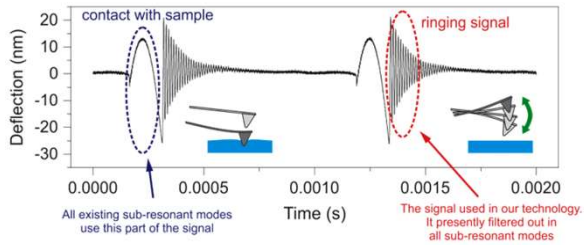
UMONS
Université de Mons







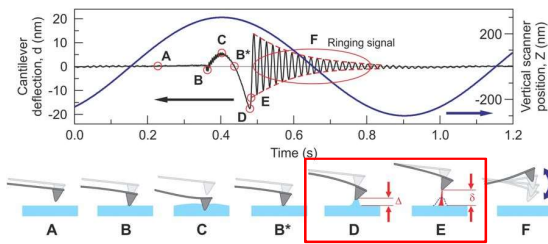
Ringing Mode ...



Scientific Reports 7, Article number: 11828 (2017)

UMONS
Université de Mons

Ringing Mode ...



Scientific Reports 7, Article number: 11828 (2017)

UMONS
Université de Mons

Ringing Mode

Why Ringing mode?

	Contact/DC	Tapping/AC	Sub-resonance	Ringing
# of channels	3	3/4	6	6+8
Description	Height, error, friction	Height, amplitude, Phase (deflection)	Height, error, adhesion, Stiffness, Visc. Losses, Deformation	All sub-resonance + 8 more
Physical channels to unambiguously characterize materials	2	1	5	5+7



Scientific Reports 7, Article number: 11828 (2017)

UMONS
Université de Mons

Ringing Mode

Why Ringing mode?

	Contact/DC	Tapping/AC	Sub-resonance	Ringing
# of channels	3	3/4	6	6+8
Description	Height, error, friction	Height, amplitude, Phase (deflection)	Height, error, adhesion, Stiffness, Visc. Losses, Deformation	All sub-resonance + 8 more
Physical channels to unambiguously characterize materials	2	1	5	5+7



Scientific Reports 7, Article number: 11828 (2017)



Ringing Mode

New Data Channels of Ringing Mode

1. Restored (averaged) adhesion
2. Adhesion height
3. Disconnection height
4. Zero-force height (*)
5. Pull-off neck height
6. Disconnection distance
7. Disconnection energy loss
8. Dynamic creep phase shift

(*) This channel, though, is available in some commercial AFMs.

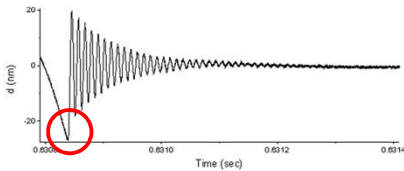


Scientific Reports 7, Article number: 11828 (2017)



Ringing Mode

1. Restored (averaged) adhesion



$$Aver F_{Re} = \frac{1}{N} \sum_{k=1}^N \frac{\text{cantilever rebound signal}}{\text{Exp}(-\pi f_0 t_k / Q) |\text{Sin}(2\pi f_0 t_k + \varphi)|}$$

The image above is a self-explanatory definition of **averaged restored adhesion**. Because the ringing signal is proportional to the original adhesion (pull-off force), it can be "restored" using the formula shown above.



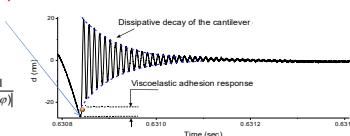
Scientific Reports 7, Article number: 11828 (2017)



Ringing Mode

1. Restored (averaged) adhesion

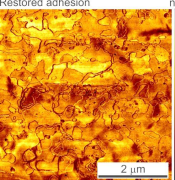
Formula to calculate:

$$Aver F_{\text{res}} = \frac{1}{N} \sum_{i=1}^N \frac{\text{cantilever rebound signal}}{\text{Exp}(-\pi f_{\text{res}} / Q) [\sin(2\pi f_{\text{res}} t + \phi)]}$$


Less noise due to multiple averaging:
Ringing rest. adhesion
vs
Regular adhesion in PeakForce Tapping

Ringing mode

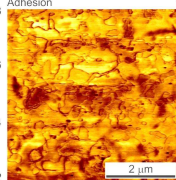
Restored adhesion



2 μm

PeakForce Tapping

Adhesion



2 μm

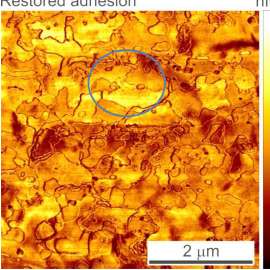
UMONS
Scientific Reports 7, Article number: 11828 (2017)

Ringing Mode

1. Restored (averaged) adhesion

Ringing mode

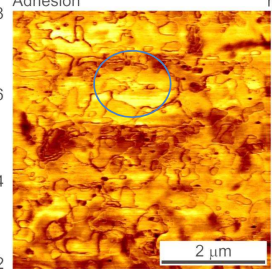
Restored adhesion



2 μm

PeakForce Tapping

Adhesion



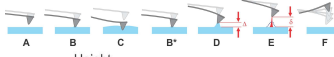
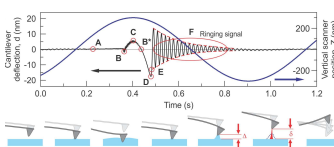
2 μm

Note: both channels are recorded simultaneously

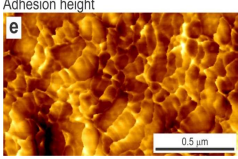
UMONS
Scientific Reports 7, Article number: 11828 (2017)

Ringing Mode

2. Adhesion height

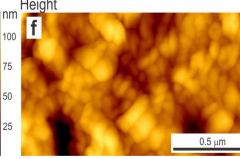


Adhesion height



0.5 μm

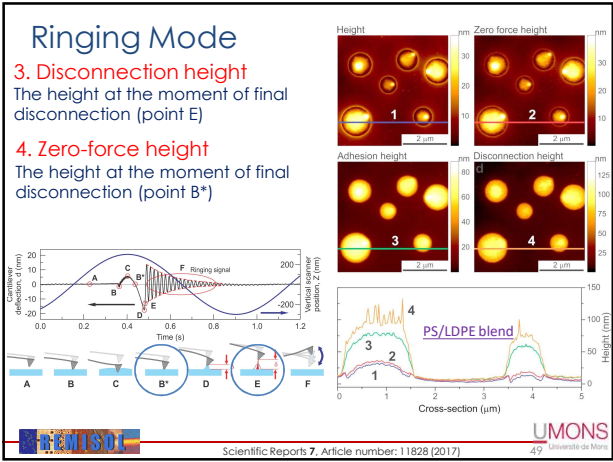
Height

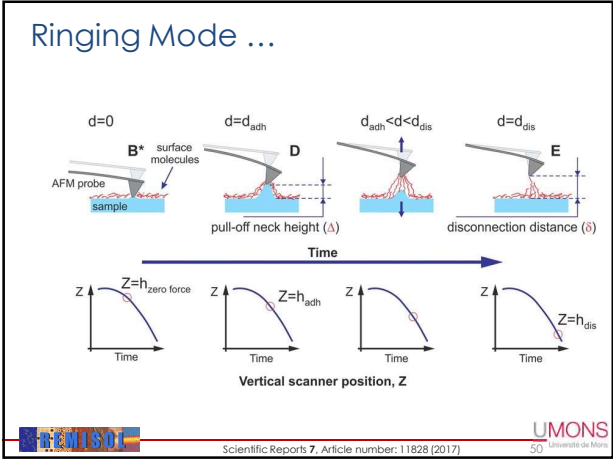


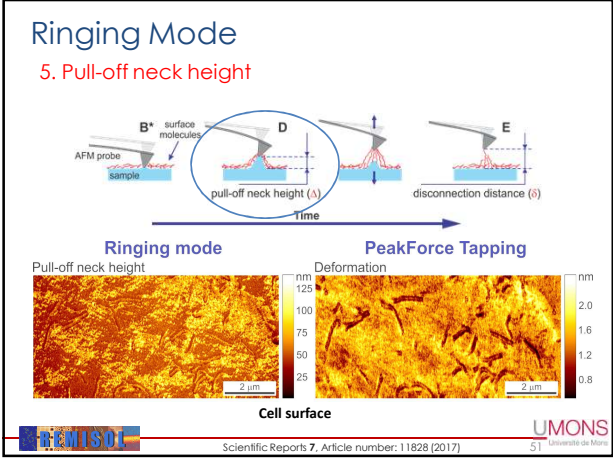
0.5 μm

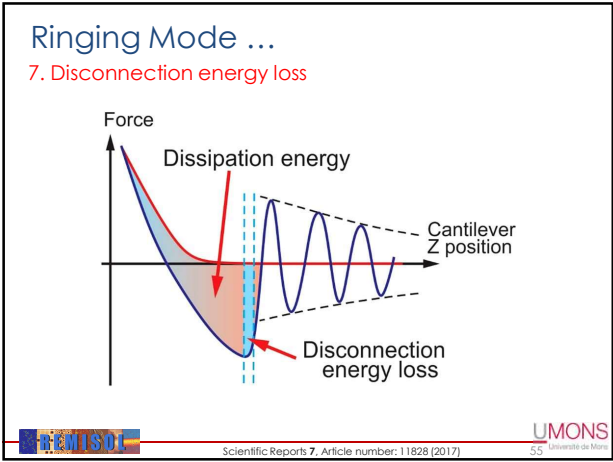
A375 human melanoma cells

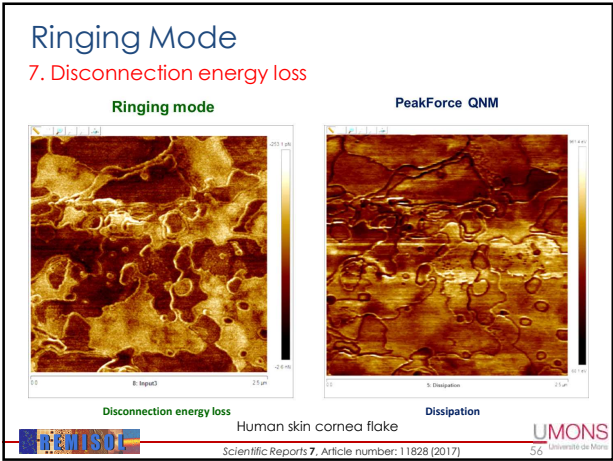
UMONS
Scientific Reports 7, Article number: 11828 (2017)

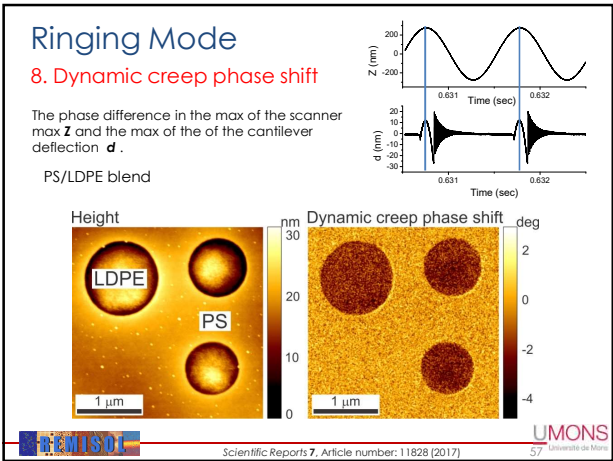


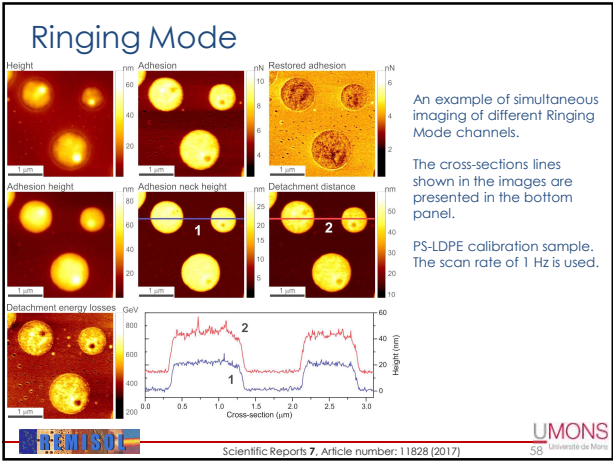


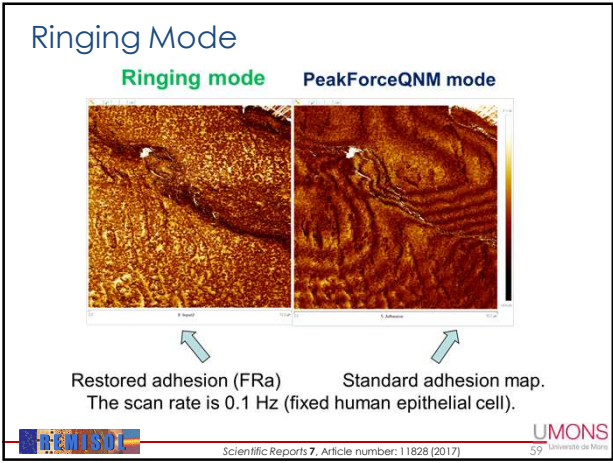








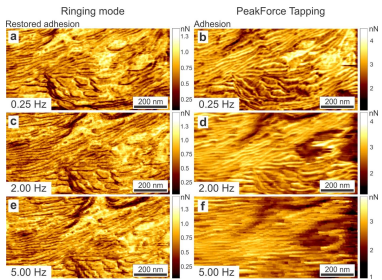






Ringing Mode

Advantage: Speed



Comparison of the restored adhesion (a,c,e; left column) and adhesion images (b,d,f; right column) obtained with ringing and PeakForce Tapping modes, respectively, recorded at different scanning speeds.

Maps of polystyrene-polycaprolactone composite polymeric material are shown.



UMONS
Université de Mons

Multifrequency AFM

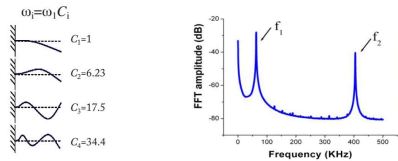
Bimodal AFM = Dual AC Mode

APPLIED PHYSICS LETTERS VOLUME 84, NUMBER 3 19 JANUARY 2004

Compositional mapping of surfaces in atomic force microscopy by excitation of the second normal mode of the microcantilever

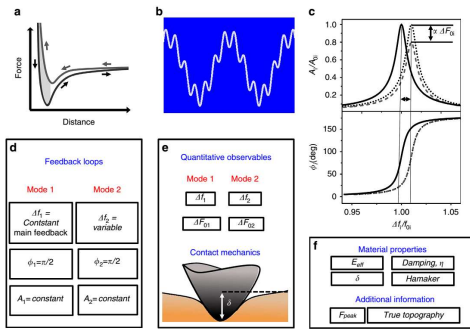
Tomás R. Rodríguez and Ricardo García¹
¹Instituto de Microelectrónica de Madrid, CSIC, Isaac Newton 8, 28760 Tres Cantos, Madrid, Spain
(Received 4 August 2003; accepted 20 November 2003)

We propose a method for mapping the composition of a surface by using an amplitude modulation atomic force microscope operated without tip-surface mechanical contact. The method consists in exciting the first two modes of the microcantilever. The nonlinear dynamics of the tip motion, the coupling of its first two modes, and its sensitivity to low-range attractive forces allows us to use this mode to probe compositional changes while the signal from the first mode is used to image the sample surface. We demonstrate that the second mode has a sensitivity to surface force variations below 10^{-14} N. © 2004 American Institute of Physics.
[DOI: 10.1063/1.1642275]



UMONS
Université de Mons

Bimodal AFM = Dual AC Mode



UMONS
Université de Mons

Bimodal AFM = Dual AC Mode

$$\Delta f_i(d_m) = -\frac{f_0}{k_i} \frac{\langle F_{0i} z_i \rangle_{T_i}}{A_i^2} = -\frac{f_0}{k_i - A_i^2} \frac{1}{T_i} \int_{T_i - \frac{\pi}{2}}^{T_i + \frac{\pi}{2}} F_{0i}(z_i - z_1 - z_2) z_i dt$$

$$d_m = z_c - A_1 - A_2$$

$$\Delta f_1(d_m) = \frac{f_1}{k_1 \sqrt{2\pi A_1}} I_1^{1/2} F(d_m)$$

$$I_1^{1/2} F(z) = \frac{1}{\Gamma(1/2)} \int_z^\infty \frac{F(t)}{(t-z)^{1/2}} dt$$

$$\Delta f_2(d_m) = \frac{f_2}{2k_2 \sqrt{2\pi A_1}} D_1^{1/2} F(d_m)$$

$$D_1^{1/2} F(z) = \frac{(-1)}{\Gamma(1/2)} \frac{d}{dz} \int_z^\infty \frac{F(t)}{(t-z)^{1/2}} dt$$

Young's Modulus

$$\Delta f_1(d_m) = \sqrt{\frac{R}{8A_1^3}} \frac{f_0}{k_1} E_{eff} \delta^2 = \beta_1 E_{eff} \delta^2$$

Viscosity

$$\Delta F_{01}(d_m) = F_{01} \left(\frac{\Delta f_1(d_m)}{f_1} + \frac{\sqrt{2\pi} Q_1 f_1}{k_1 A_1^{3/2}} I_1^{1/2} B(d_m) \right)$$

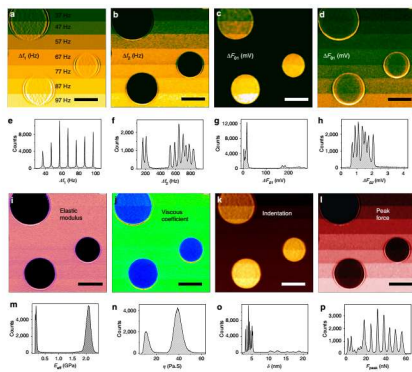
$$\Delta f_2(d_m) = \sqrt{\frac{R}{8A_1^3}} \frac{f_0}{k_2} E_{eff} \delta = \beta_2 E_{eff} \delta$$

$$B(x) = 2 \int \eta \sqrt{R} \delta dx$$

$$I_1^{1/2} B(d_m) = 0.5 \sqrt{\pi R} \eta \delta^2$$

UMONS
Université de Mons

Bimodal AFM = Dual AC Mode

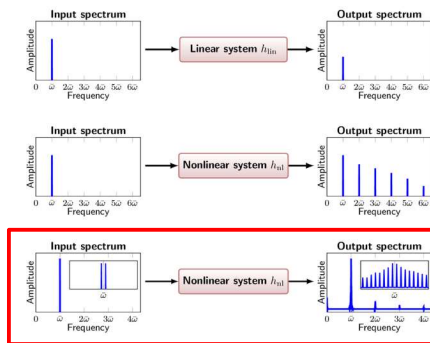


UMONS
Université de Mons

Intermodulation AFM

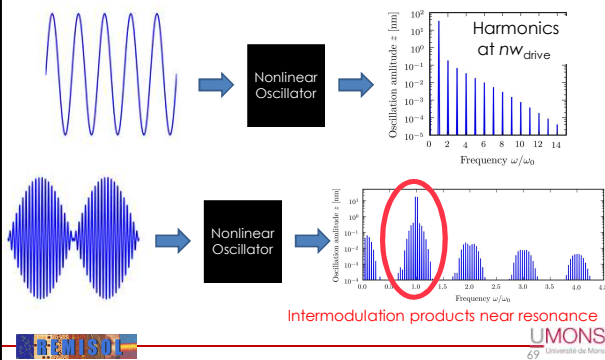
The methodology

Intermodulation AFM



UMONS
Université de Mons

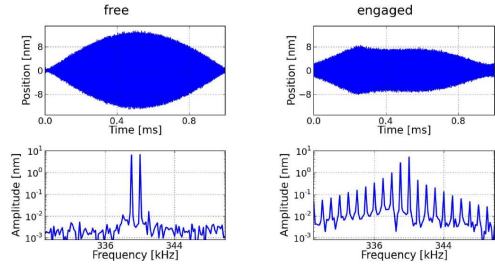
Harmonics, Intermodulation AFM



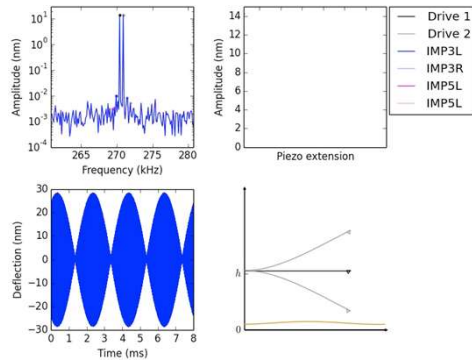
UMONS
Université de Mons

Intermodulation AFM

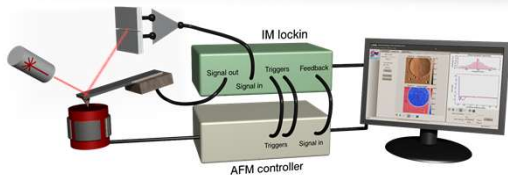
- Cantilever driven with two pure drive tones close to resonance
- Nonlinear tip-surface force creates new components in the spectrum (Intermodulation products)



Intermodulation AFM



Intermodulation AFM

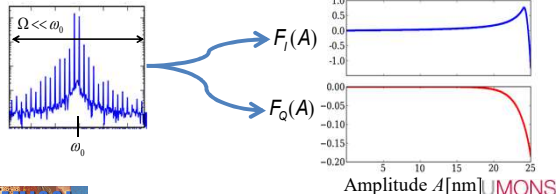


Force Quadratures

tip motion: $z(t) \cong h + A \cos(\omega_0 t)$

in-phase (conservative): $F_I(A) = \int_0^{2\pi} F_{ts}(z, \dot{z}) \cos(\omega_0 t) dt$

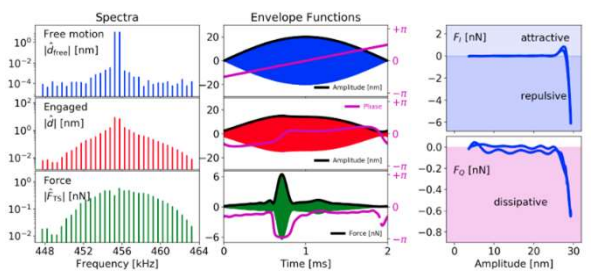
quadrature (dissipative): $F_Q(A) = \int_0^{2\pi} F_{ts}(z, \dot{z}) \sin(\omega_0 t) dt$



D. Platz et al. Nature Comm. (2012)

73 Université de Mons

Force Quadratures

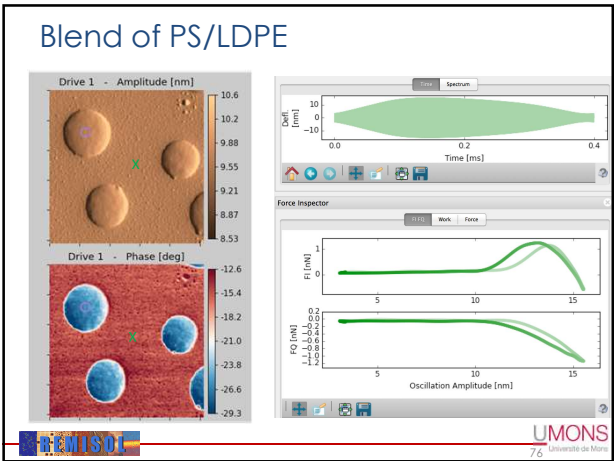


UMONS
74 Université de Mons

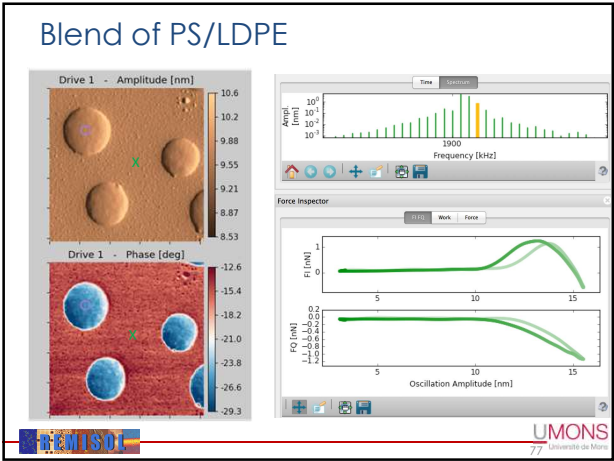
Intermodulation AFM

Some results

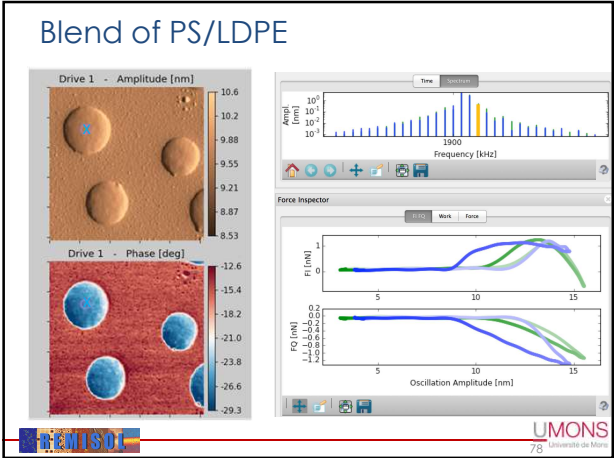
Blend of PS/LDPE

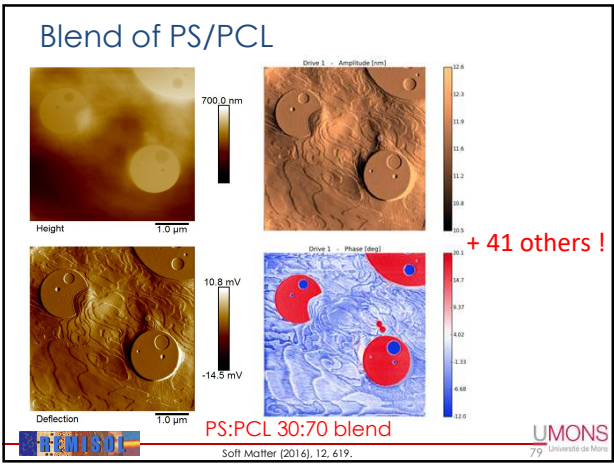


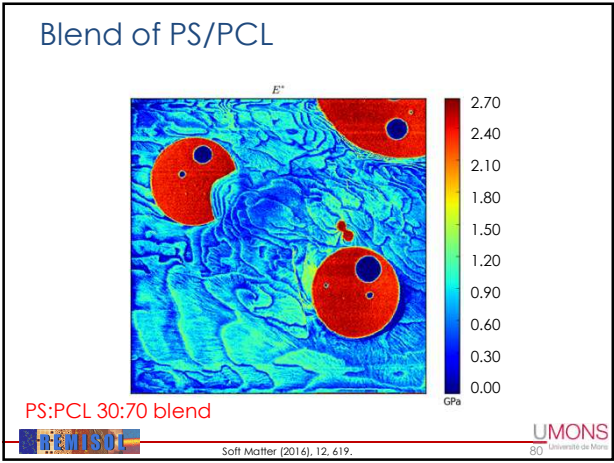
Blend of PS/LDPE

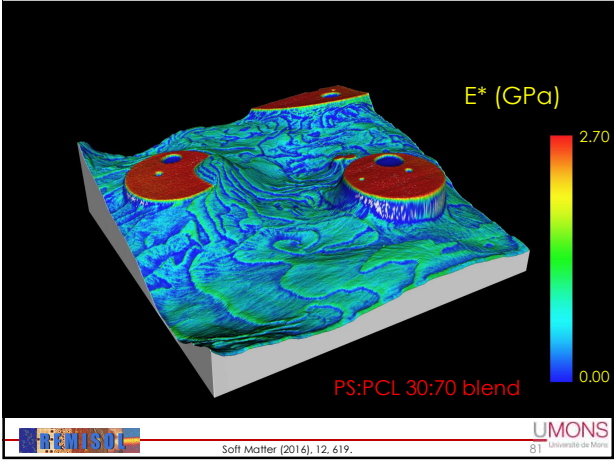


Blend of PS/LDPE

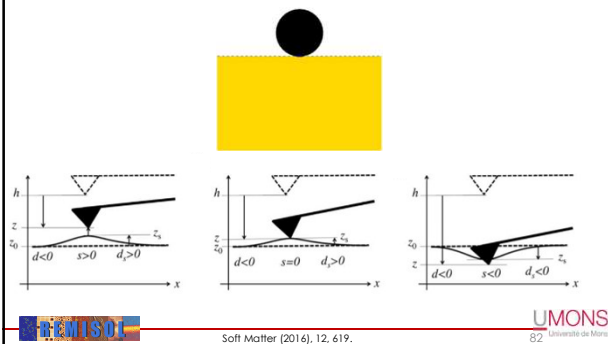








Moving surface Model



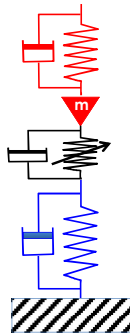
Moving surface Model

$$m\ddot{d} + \gamma m\dot{d} + kd = F_{TS}(s, \dot{s}) + F_{\text{drive}}$$

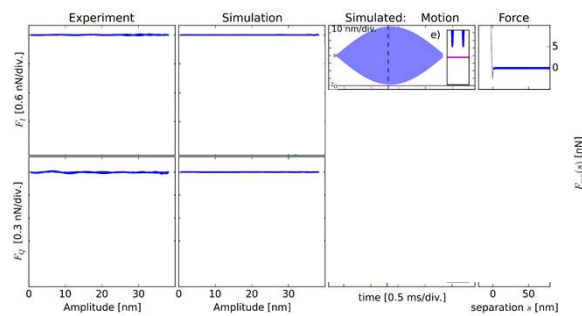
$$\eta \dot{d}_s + k_s d_s = -F_{TS}(s, \dot{s})$$

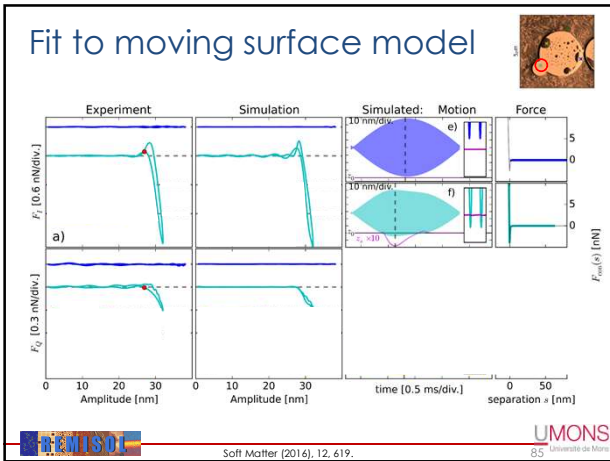
$$\text{separation } s = (d - d_s) + h - z_0$$

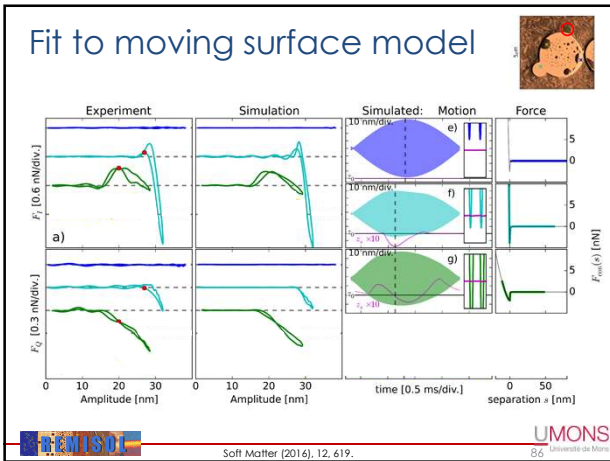
$$F_{TS}(s, \dot{s}) = \begin{cases} 0 & \text{if } s > 0 \\ -F_{\text{ad}} - k_v s - \eta_v \dot{s} & \text{if } s \leq 0 \end{cases}$$

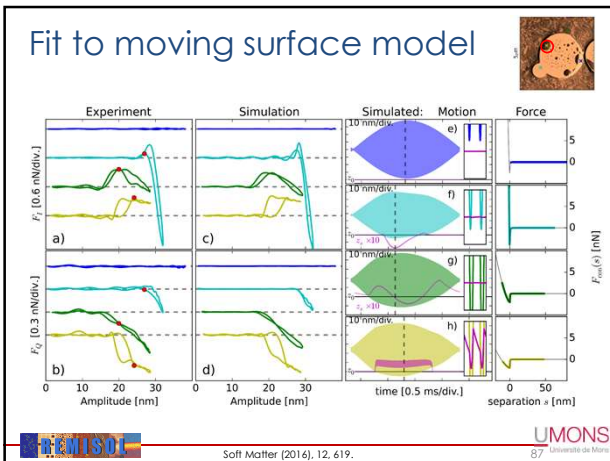


Fit to moving surface model





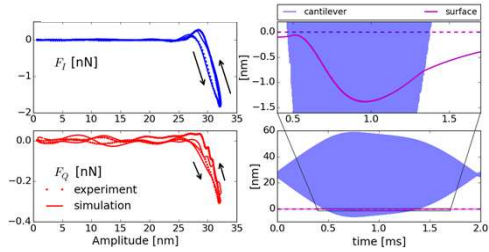




Fit to moving surface model



PS phase



surface stiffness $k_s = 5.35 \cdot 10^3$ [N/m]
surface time constant $\tau_s = \eta_s / k_s = 5.4 \cdot 10^{-4}$ [s]



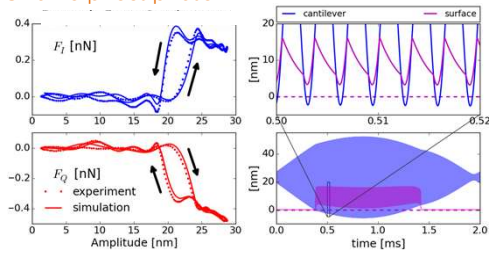
Soft Matter (2016), 12, 619.

UMONS
Université de Mons

Fit to moving surface model



PCL amorphous phase



surface stiffness $k_s = 5.10 \cdot 10^3$ [N/m]
surface time constant $\tau_s = \eta_s / k_s = 1.8 \cdot 10^{-4}$ [s]



Soft Matter (2016), 12, 619.

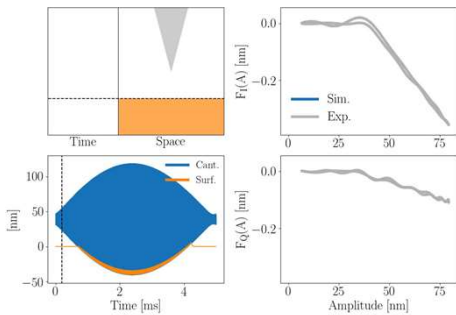
UMONS
Université de Mons

Fit to moving surface model

Courtesy of P.A. Thoren

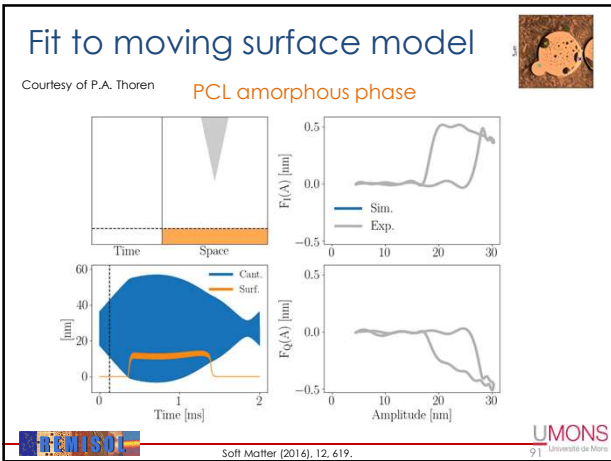


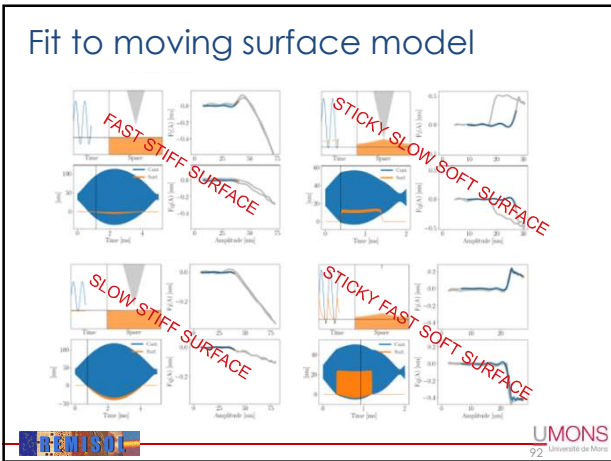
PS phase

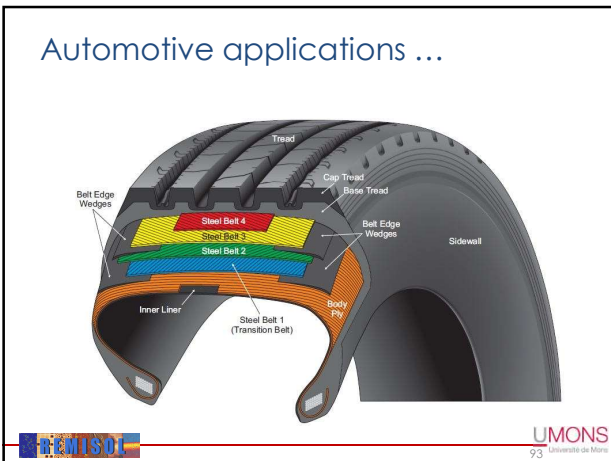


Soft Matter (2016), 12, 619.

UMONS
Université de Mons







DVA Inner layer



The inner liner is an extruded rubber sheet compounded with additives that result in low air permeability. The inner liner assures that the tire will hold high-pressure air inside, without the air gradually diffusing through the rubber structure.

The inner layer of the tire is made with DVA (Dynamically Vulcanized Alloy,) a technology developed by ExxonMobil Chemical, to increase the IPR (Inflation Pressure Retention – used to measure of tire air pressure loss over time), more efficiently than regular tires.

The sample used in this study is a DVA of rubber domains (Brominated Poly(Isobutylene-co-p-Methylstyrene), BIMS) dispersed in a polyamide (PA, also referred to as nylon) continuous phase.

The sample was cryomicrotomed.

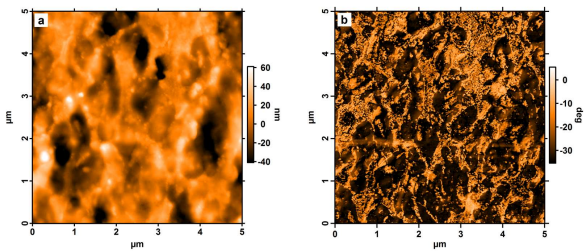


Polymer 135 (2018), 348-354

UMONS
94 Université de Mons

DVA Inner layer

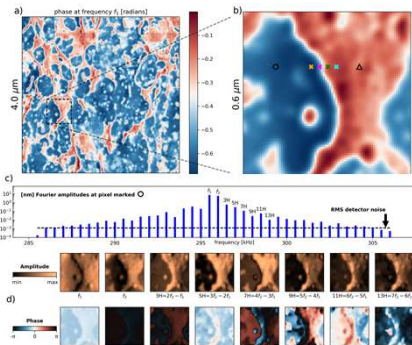
Tapping Mode AFM



Polymer 135 (2018), 348-354

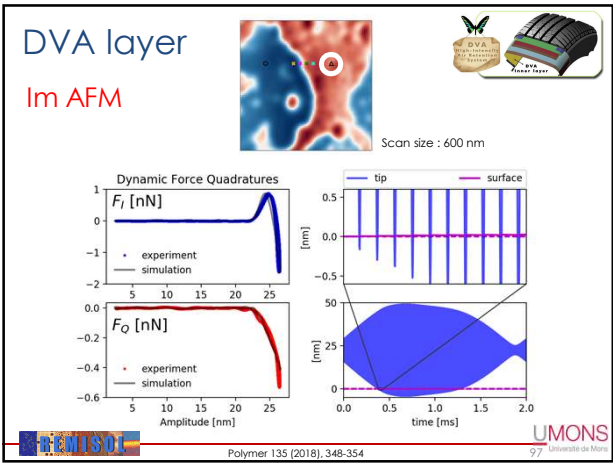
UMONS
95 Université de Mons

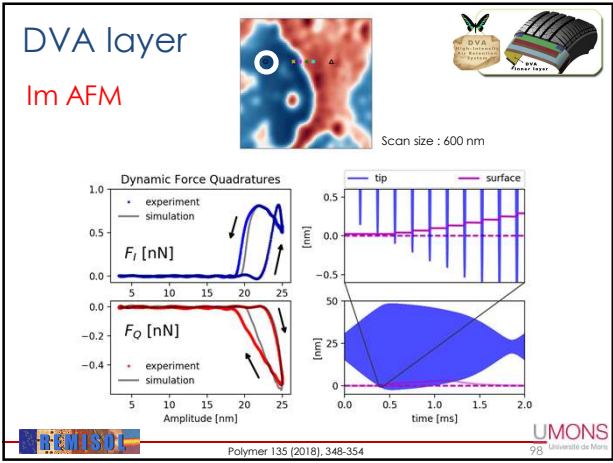
DVA Inner layer

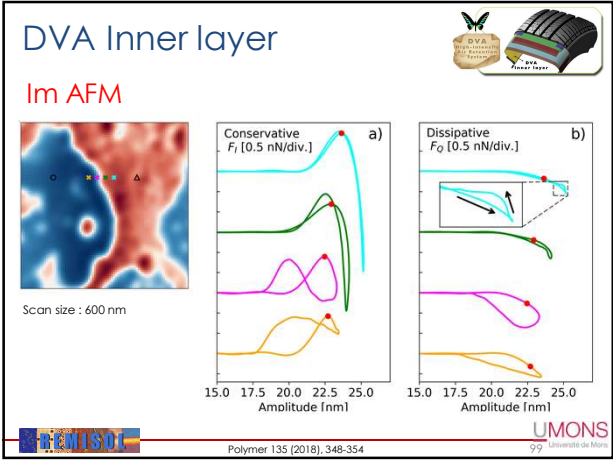


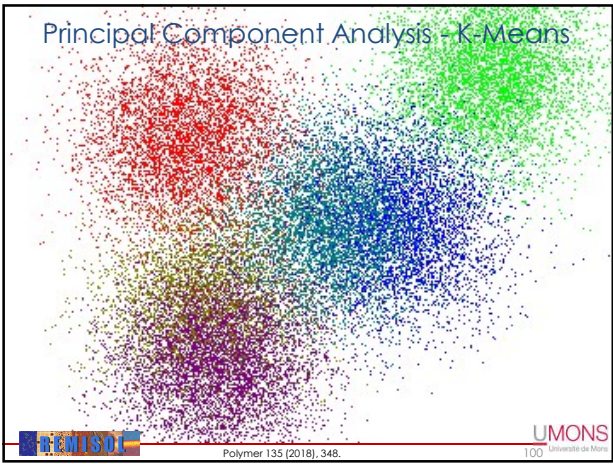
Polymer 135 (2018), 348-354

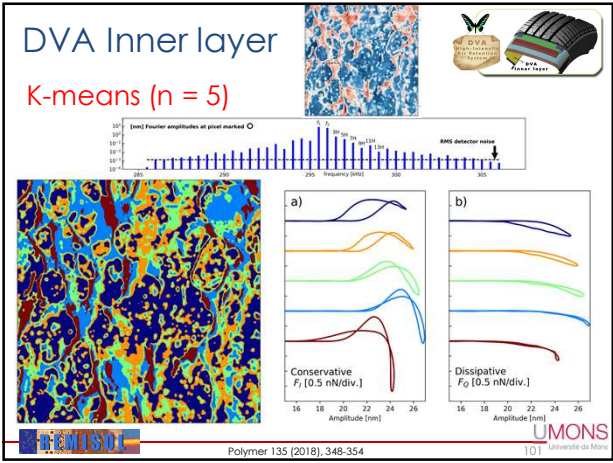
UMONS
96 Université de Mons

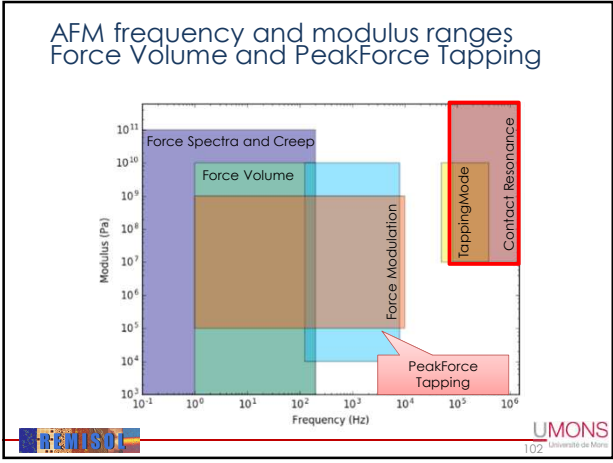




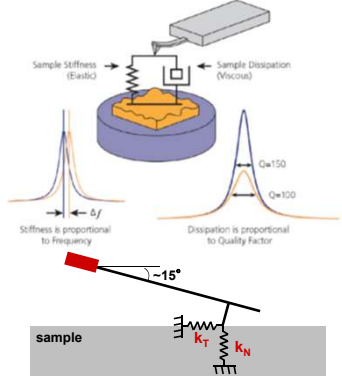








Contact Resonance



Adapted from Asylum Research

UMONS
103 Université de Mons

How to measure Frequency & Q ?

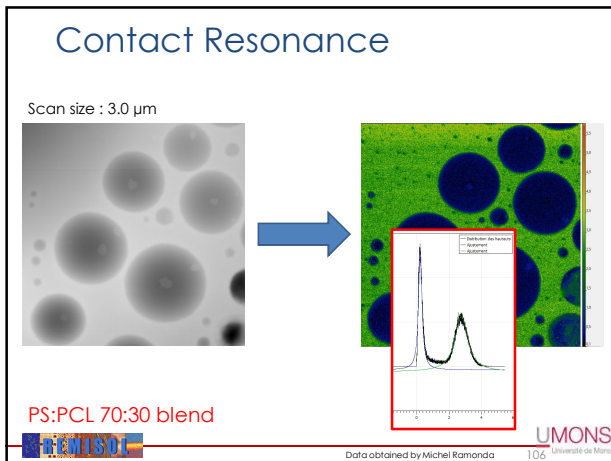
Measuring the resonance frequency

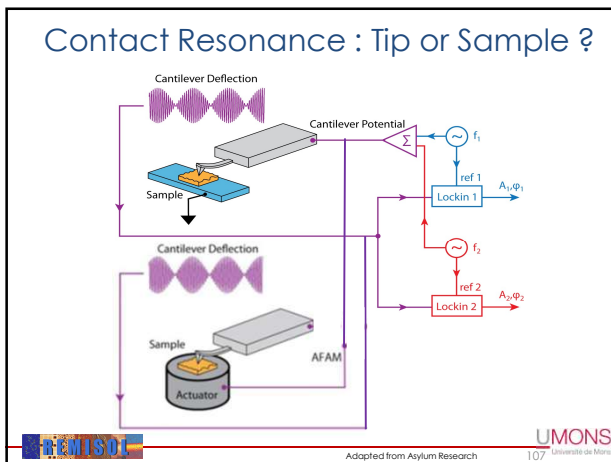
Methods	What it does	Benefits	Disadvantages
Fixed frequency ²	The cantilever response is measured at a fixed frequency, which varies as the contact resonance frequency shifts.	Simple to implement and produces elastic contrast images.	Produces only qualitative results since the frequency shift itself is not measured. Contrast is lost if the peak shifts too far from the selected frequency.
PLL frequency tracking ¹	A phase-locked loop (PLL) uses the phase of the cantilever response to track the contact resonance frequency.	The actual contact resonance frequency is tracked.	Difficult to tune the PLL to achieve stable frequency tracking due to spurious phase shifts in the response. Does not measure the Q of the resonance.
Frequency sweep (chirp) ^{3,4,5}	A frequency sweep (chirp) is done at each point. The cantilever response is Fourier analyzed to recover the full frequency response.	Measures the entire frequency response, so both the frequency and Q are obtained. Additional analysis is possible based on more complex models.	Mapping is quite slow when collecting large numbers of pixels. Each sweep must be done slowly enough for the cantilever to respond (rate limited by Q).
DART ^{6,7,8} (DRFT)	The amplitude and phase response at two frequencies (bracketing the contact resonance) is measured, which enables the contact resonance to be tracked.	Provides both the contact resonance frequency and Q. The tracking is extremely fast, so DART imaging can be done at normal imaging rates.	The full response is not measured, so analysis is more limited than frequency sweep or band excitation methods.
Band Excitation ^{8,9}	A continuous band of frequencies is excited. The cantilever response is Fourier analyzed to recover the full frequency response.	The entire frequency response is measured. By exciting the entire band at once, it is much faster than other full spectrum techniques (e.g. sweep).	Data transfer bandwidth limitations make the current implementation significantly slower than DART. Future speed improvements are possible.

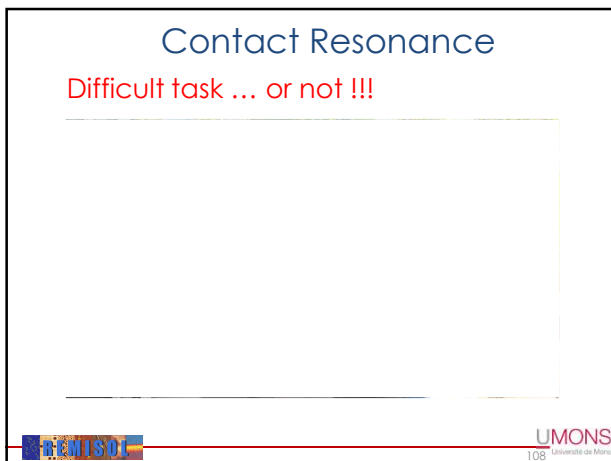


From Asylum Research (CR-AFM application note)

UMONS
105 Université de Mons







Recent developments in data processing ...

Big, Deep, Smart Data !!!

Recent modes further expand these capabilities by enabling the acquisition of multidimensional data cubes. For materials scientists and engineers, this breaks long-standing efficiency and characterization barriers. These new capabilities provide simultaneous capture of nanometer-scale mechanical (and electrical) characteristics in **high-density data cubes**, previously impossible to attain in a single measurement.



Data processing ...

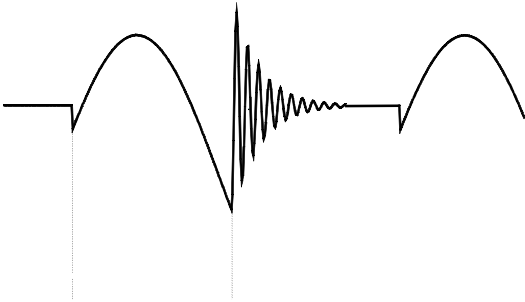
Mechanical Properties

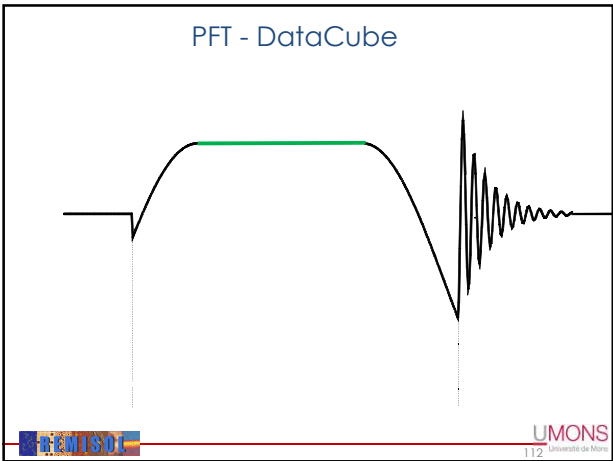
Techniques	Benefits
DataCube Mode	Multidimensional data cube Soft and fragile matter Correlation to mechanical properties
PeakForce Tapping	Soft and fragile matter Correlation to mechanical properties
Tapping Mode	First technique available
Contact Mode	First technique available

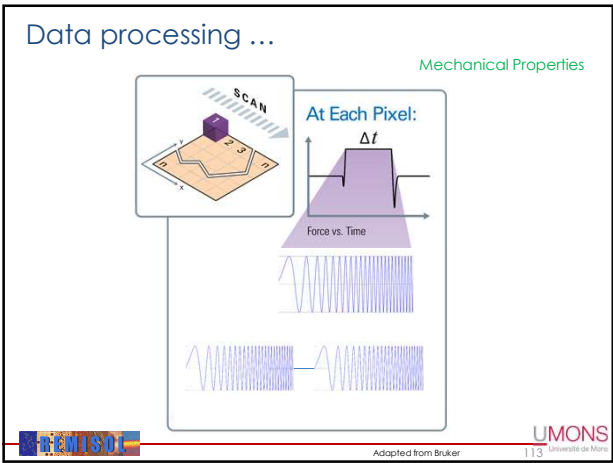


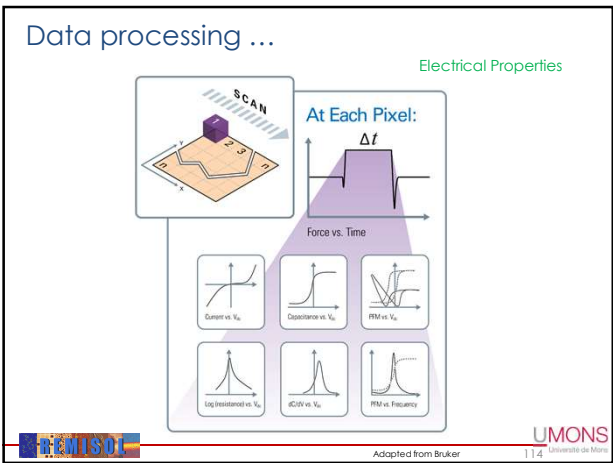
Adapted from Bruker

Back to Sub Resonance Tapping ...



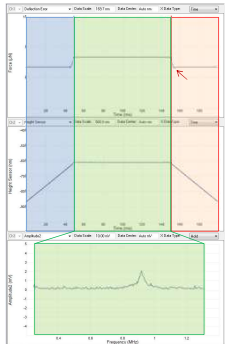






Peak Force Tapping - Contact Resonance

- CR is based on FASTForce Volume
 - Provides standard force curve for comparison for each pixel in map
 - Approach
 - Hold Force and sweep frequency
 - Retract
 - **More repeatable:** lateral force on tip is minimized, reducing tip wear
 - **More information:** allows measurement of adhesion force for each pixel better contact mechanics modelling
 - **Real-time maps** of both raw data and mechanical props (E^* , E'' , loss tan)
 - **Whole sweep is saved**, allowing detection of artifact peaks, etc. (unlike frequency tracking methods like DA(F)RT)

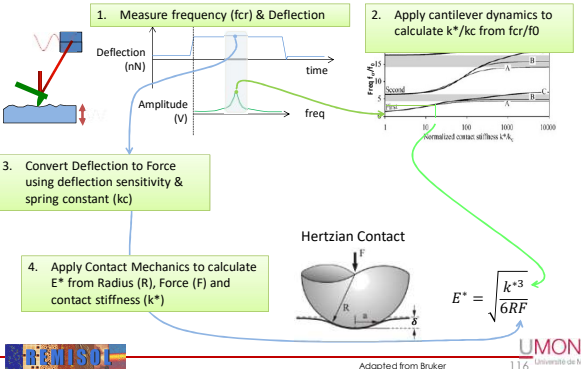


Adapted from Bruker

UMONS
Université de Mons

Contact Resonance

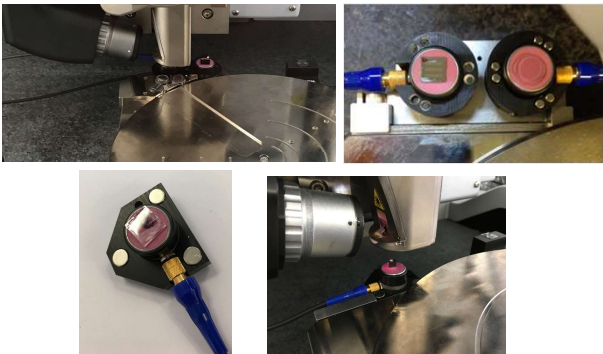
From Frequency and Deflection to modulus



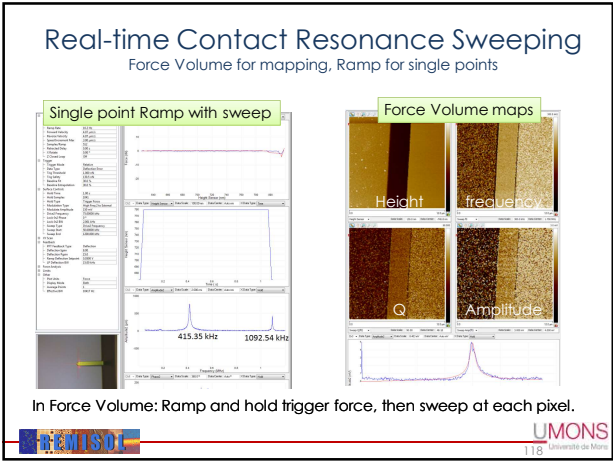
Adapted from Bruker

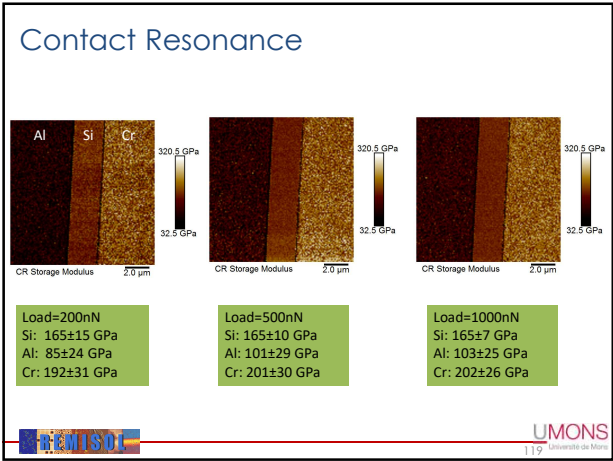
UMONS
Université de Mons

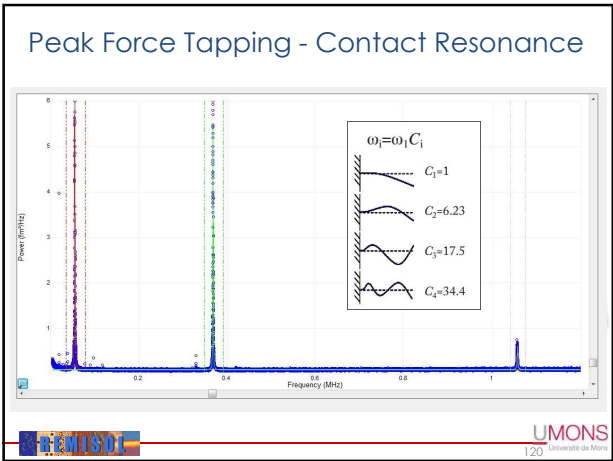
Peak Force Tapping Contact Resonance

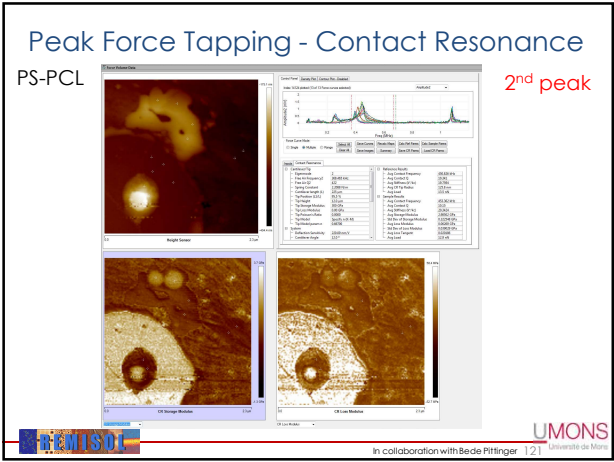


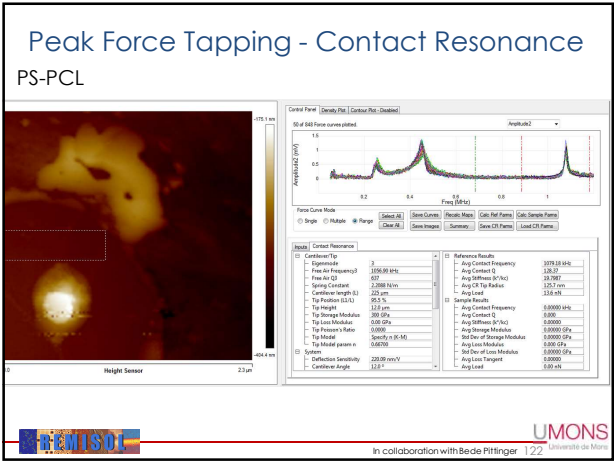
UMONS
Université de Mons

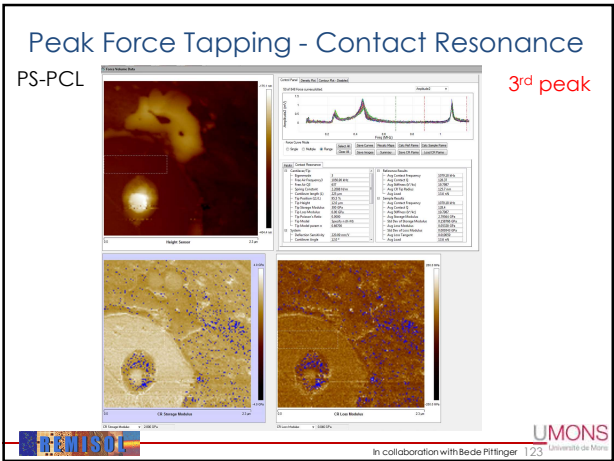












Peak Force Tapping - Contact Resonance

PS-PCL



UMONS
In collaboration with Bede Pittinger 124 Université de Mons

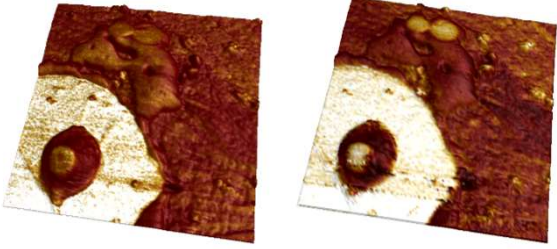
Peak Force Tapping - Contact Resonance



UMONS
In collaboration with Bede Pittinger 125 Université de Mons

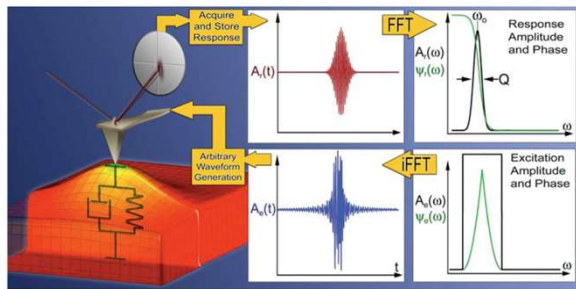
Comparing PFTQNM and CR

- PFTQNM
- CR 128x128



UMONS
In collaboration with Bede Pittinger 126 Université de Mons

Band Excitation (BE)



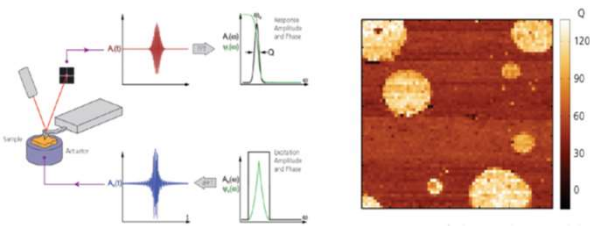
And Google Mode SPM ...

S. Jesse, S.V. Kalinin, R. Proksch, A.P. Baddorf, and B.J. Rodriguez, Nanotechnology 18, 435503 (2007).



UMONS
Université de Mons

Band Excitation (BE)



UMONS
Université de Mons

Conclusions

Conclusions

SPM is a powerful characterization tool for polymer science, capable of revealing surface structures with high resolution and provides useful information on the morphology of polymeric materials ... complementary to other techniques.

Force distance curve analysis allow multiple material properties to be decoupled and measured independently ... even of very soft materials !

For instance, recording mechanical properties and adhesion maps in parallel to topography and phase images is now possible with quantitative SPM.

New methods (such as PFT) are able to « rapidly » map the mechanical properties at the nanometer scale due to the high acquisition and analysis processes.



Conclusions

• **Combined, AFM measurements with non-resonant modes and resonant modes can provide**

- Huge range of properties covered
- FV based Contact Resonance for stiff samples at higher frequencies
- FV force curves for soft samples at low frequencies
- FV and PFT cover wide range of ramp rates for time-temperature studies

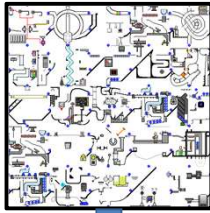
• **Understanding the relative contribution of the various error sources allows us to prioritize improvements to address them**

- Spring constant and tip shape are key parameters for all of the methods
- Force Volume can have fairly high accuracy if k and R are well known, PFT is not quite as accurate, but is often worth using for resolution and speed
- Contact resonance has a lot of parameters that need to be calibrated, making 'relative' measurements more practical than 'absolute'
- Appropriate modeling is required to quantify the modulus depending on the sample and measurement conditions



Conclusions

Multifrequency methods are extremely promising but also need some (new) models to provide quantitative parameters. Data-driven materials development and design (Machine learning, AI) are most probably the key issue to achieve this goal.



Property mapping



